

Origin of ferromagnetism in Fe- and Cu-codoped ZnO

Jeong Hyun Shim,^{a)} Taesoon Hwang, and Soonchil Lee

Department of Physics, Korea Advanced Institute of Science and Technology, Daejeon 305-701, Republic of Korea

Jung Hye Park, Seung-Jin Han, and Y. H. Jeong

Department of Physics and Electron Spin Science Center, Pohang University of Science and Technology, Pohang 790-784, Republic of Korea

(Received 25 October 2004; accepted 5 January 2005; published online 15 February 2005)

Fe- and Cu-codoped ZnO was previously reported as a room-temperature dilute magnetic semiconductor. We have investigated the origin of the ferromagnetism in $\text{Zn}_{0.95-x}\text{Fe}_{0.05}\text{Cu}_x\text{O}$ using the zero-field ^{57}Fe nuclear magnetic resonance and neutron diffraction. These measurements reveal that some Fe ions of $\text{Zn}_{0.95-x}\text{Fe}_{0.05}\text{Cu}_x\text{O}$ form a secondary phase, ZnFe_2O_4 . Detailed comparison of nuclear magnetic resonance spectra of $\text{Zn}_{0.95-x}\text{Fe}_{0.05}\text{Cu}_x\text{O}$, bulk ZnFe_2O_4 with normal spinel structure, and nanocrystalline ZnFe_2O_4 with inverted spinel structure shows that the secondary phase possesses an inverted spinel structure and is ferrimagnetic at room temperature, while normal zinc ferrite is nonmagnetic. The ferromagnetism in Fe- and Cu-codoped ZnO stems from the secondary phase, while the majority of Fe ions substituted into the ZnO lattice appears to remain magnetically inert. © 2005 American Institute of Physics. [DOI: 10.1063/1.1868872]

Recently, ferromagnetic semiconductors have been actively pursued because of their potential as spin-polarized carrier sources and easy integration into semiconductor devices.¹

One obvious way to make ferromagnetic semiconductors is to dope semiconductors with magnetic impurities. A well-known example of these dilute magnetic semiconductors is GaMnAs with transition temperature (T_c) of 110 K, well below room temperature.² A theoretical work using a mean-field model predicted ferromagnetism above room temperature in a II-VI semiconductor ZnO when doped with holes and Mn.³ ZnO, which also possesses excellent optical properties, received attention, and several reports on ZnO doped with transition metal ions followed.⁴ These studies, however, did not lead to consistent conclusions. Ferromagnetism was observed at room temperature for Co-doped ZnO films but reproducibility was quite low.⁵ Evidence that the magnetic property of Mn-doped ZnO films is extrinsic, that is, due to the unintentionally produced magnetic impurity phases, now exists.⁶ Fe-doped bulk ZnO even shows antiferromagnetism, rather than ferromagnetism, at low temperatures.⁷

It was reported previously that additional doping of Cu into Fe-doped ZnO generates ferromagnetism with $T_c = 550$ K;⁸ Cu was introduced as a p -type dopant in naturally n -type ZnO. High transition temperature and high reproducibility made the material look quite promising. However, high-resolution x-ray diffraction measurements also revealed tiny extra peaks in addition to the main ones belonging to the hexagonal lattice of ZnO. (The majority of doped Fe ions were incorporated into the lattice.) These tiny peaks were identified as belonging to ZnFe_2O_4 , which is normally nonmagnetic at room temperature. It was also found that the magnetization of $\text{Zn}_{0.95-x}\text{Fe}_{0.05}\text{Cu}_x\text{O}$ increases with Cu concentration up to 1.0%, where it starts to decrease on further doping, while the amount of ZnFe_2O_4 increases monotonically past 1.0%. This observation and the attribute that

ZnFe_2O_4 is nonmagnetic, among others, led us to conclude that the ferromagnetism of $\text{Zn}_{0.95-x}\text{Fe}_{0.05}\text{Cu}_x\text{O}$ is an intrinsic property.

However, it is known that ZnFe_2O_4 with inverted spinel structure can become ferrimagnetic,⁹ and therefore the possibility that the ferromagnetism seen in $\text{Zn}_{0.95-x}\text{Fe}_{0.05}\text{Cu}_x\text{O}$ is due to the secondary phase is not completely excluded. In this study, we address this issue and investigate the origin of the ferromagnetism of $\text{Zn}_{0.95-x}\text{Fe}_{0.05}\text{Cu}_x\text{O}$ more carefully using zero-field NMR and neutron diffraction. The main conclusion drawn from the present experimental study is that the ferromagnetism of $\text{Zn}_{0.95-x}\text{Fe}_{0.05}\text{Cu}_x\text{O}$ is not due to the diluted interacting Fe ions in the lattice, but is due to the small amount of the secondary magnetic phase, inverted spinel ZnFe_2O_4 .

Whether the magnetic property of a material is intrinsic cannot be determined by measurements of macroscopic quantities such as magnetization or conductivity. It requires a local probe such as NMR; the resonance frequency of NMR is proportional to the total field that a local nucleus sees. An NMR spectrum obtained at zero external field for magnetic materials reflects the local hyperfine field that contains all the information about the local electronic state and configuration of a specific magnetic atom. Thus, NMR and neutron diffraction, whose spectrum is also sensitive to magnetic ordering, were employed in this study. High-resolution neutron powder diffraction was carried out at the HANARO reactor in KAERI. ^{57}Fe NMR spectra were obtained at zero external field by using our homemade spectrometer carefully tuned to give the maximum signal-to-noise ratio at low temperatures. Because of the low natural abundance of iron, data were taken only at 4 K by the spin echo technique.

Polycrystalline samples of bulk $\text{Zn}_{0.95-x}\text{Fe}_{0.05}\text{Cu}_x\text{O}$ were fabricated with the standard solid state reaction method, as described previously.⁸ The neutron diffraction spectrum of $\text{Zn}_{0.94}\text{Fe}_{0.05}\text{Cu}_{0.01}\text{O}$ is plotted in Fig. 1; the minor peaks from ZnFe_2O_4 are indicated in the figure. The inset shows that the intensity of the peak at 21.7° , which occurs at the lowest

^{a)}Electronic mail: abehool@kaist.ac.kr

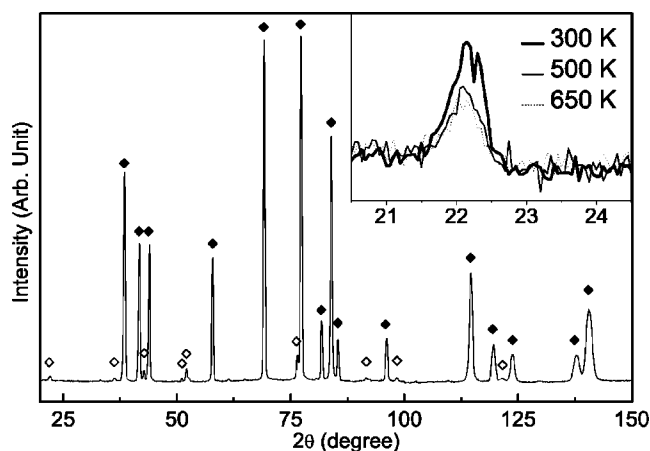


FIG. 1. The spectrum of neutron powder diffraction for $\text{Zn}_{0.94}\text{Fe}_{0.05}\text{Cu}_{0.01}\text{O}$. Solid symbols indicate the peaks from the ZnO lattice, and tiny peaks with open symbols are from ZnFe_2O_4 . Inset displays a peak from ZnFe_2O_4 as a function of temperature.

angle among the ZnFe_2O_4 Bragg peaks, increases when temperature is decreased below T_c . The peaks corresponding to the ZnO structure remain invariant irrespective of temperature variation. Neutron diffraction is caused by both crystal structure and magnetic ordering; the peak height variation below T_c would then be due to magnetic ordering. Thus, neutron data indicate that the magnetization of the impurity phase grows as temperature is reduced below T_c , and one may suspect that the magnetization of the secondary phase ZnFe_2O_4 is somehow correlated with that of the sample. However, the change of the peak height is too small to make any kind of quantitative comparison with the measured magnetization variation.

A more definite comparison was attempted by measuring the NMR spectra of $\text{Zn}_{0.95-x}\text{Fe}_{0.05}\text{Cu}_x\text{O}$ as well as normal and inverted ZnFe_2O_4 . Bulk ZnFe_2O_4 has a spinel structure where metal ions are located at interstitial sites of the close-packed fcc lattice of oxygens. There are two sites available for metal ions: tetrahedral *A* and octahedral *B*. ZnFe_2O_4 in the normal spinel structure (all Fe ions are in the *B* sites) is paramagnetic down to low temperatures, while it becomes ferrimagnetic at room temperature in the partially inverted spinel structure where some of Fe ions take *A* sites.⁹ Normal ZnFe_2O_4 is made by the solid state reaction method, while nanocrystalline ZnFe_2O_4 with inverted spinel structure can be obtained by high-energy ball-milling of the normal zinc ferrite.

The zero-field NMR spectra of $\text{Zn}_{0.95-x}\text{Fe}_{0.05}\text{Cu}_x\text{O}$ are plotted in Fig. 2 for various Cu concentrations. The experimentally determined gyromagnetic ratio confirms that this peak is the resonance signal of iron nuclei. Experimentally measured hyperfine field of a nucleus of a magnetic atom is proportional to the magnetic moment of that atom and depends on the ionic valency, configuration of neighboring atoms, bonding with neighbors, etc. Therefore, the spectrum contains information on the structure of the lattice where the ferromagnetic irons locate; the task is to clarify whether the lattice is that of ZnO or a secondary phase. No NMR signal, particularly around 71 MHz, could be detected from ZnFe_2O_4 in the normal spinel structure. The NMR spectrum of nanocrystalline ZnFe_2O_4 (ball-milled for 4 h) was measured and displayed in Fig. 2 along with the results from $\text{Zn}_{0.95-x}\text{Fe}_{0.05}\text{Cu}_x\text{O}$. The spectrum of nanocrystalline

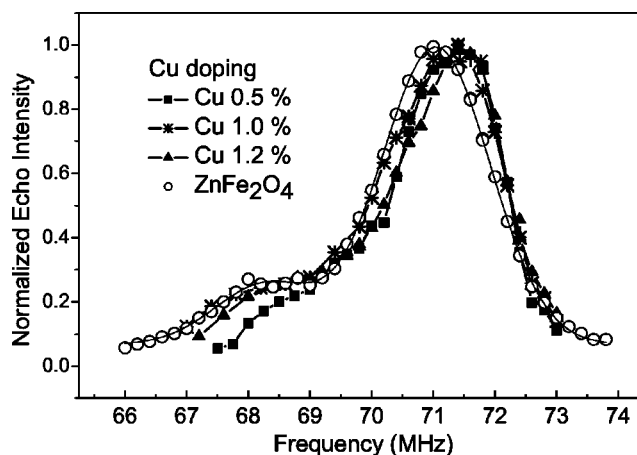


FIG. 2. The zero-field ^{57}Fe NMR spectra of $\text{Zn}_{0.95-x}\text{Fe}_{0.05}\text{Cu}_x\text{O}$ and ZnFe_2O_4 . The ZnFe_2O_4 sample was obtained by ball-milling, and was composed of nanosized grains with inverted spinel structure.

ZnFe_2O_4 again contains two peaks, one centered at 71 MHz, and another small peak centered at 68 MHz. The hyperfine fields of Fe nuclei at the *A* and *B* sites should be different because of the different structural environments, even though both Fe ions would be in the same Fe^{3+} chemical state. By observing the signal dependence on external magnetic field, we confirmed that the ball-milled ZnFe_2O_4 is indeed in a ferrimagnetic state and the high-frequency peak corresponds to the Fe atoms at the *B* site and the low-frequency peak, the *A* site.

The spectra obtained from $\text{Zn}_{0.95-x}\text{Fe}_{0.05}\text{Cu}_x\text{O}$ for various Cu concentrations are obviously identical with that of partially inverted ZnFe_2O_4 in their resonance frequency and spectral shape. Thus, it is quite clear that the spectra we observed for $\text{Zn}_{0.95-x}\text{Fe}_{0.05}\text{Cu}_x\text{O}$ originate from the iron in the secondary phase ZnFe_2O_4 produced in the sample. In most ferrites, the NMR signals of Fe^{2+} and Fe^{3+} ions are found near 40 and 70 MHz, respectively.¹⁰ The valency of Fe ions in ZnFe_2O_4 is 3+, while that of Fe ions substituting for Zn ions in ZnO is expected to be 2+.¹¹ If Fe ions substituting for Zn ions are in a ferromagnetic state, their zero-field NMR signal is expected to be found near 40 MHz. A theoretical calculation suggests a double-exchange interaction between the substituting Fe^{2+} and Fe^{3+} that is generated by charge transfer from doped Cu.¹² In that case, the average valency of Fe ions falls between 2+ and 3+ due to a rapid electron hopping process and the NMR spectrum would be found somewhere between 40 and 70 MHz. We carefully searched for the NMR signal of $\text{Zn}_{0.95-x}\text{Fe}_{0.05}\text{Cu}_x\text{O}$ from 30 to 80 MHz, but no other signal was observed except that in Fig. 2. The amount of Fe atoms forming ZnFe_2O_4 phase in $\text{Zn}_{0.95-x}\text{Fe}_{0.05}\text{Cu}_x\text{O}$ was estimated by comparing the NMR signal intensity of $\text{Zn}_{0.95-x}\text{Fe}_{0.05}\text{Cu}_x\text{O}$ with that of the ball-milled ZnFe_2O_4 . The comparison showed that the majority of Fe ions remain in the ZnO lattice, but it appears that they are magnetically inert.

In Fig. 3, the NMR resonance frequency (top) and the spectral intensity (bottom) are plotted together with the saturation magnetization obtained at 300 K as a function of Cu concentration. The resonance frequency remains the same irrespective of Cu concentration while both the NMR intensity and the magnetization are maximal at 1%. The resonance frequency ω is proportional to the hyperfine field, which in turn is proportional to the thermally averaged atomic mag-

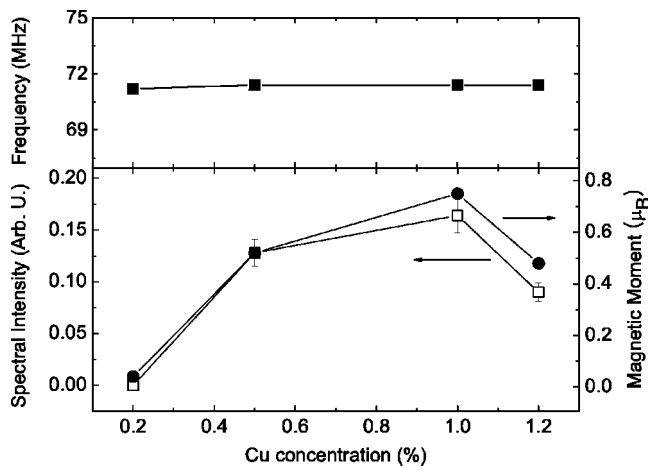


FIG. 3. The NMR resonance frequency (top), and the NMR signal intensity (bottom) are plotted as a function of Cu concentration. Also plotted in the bottom panel is the saturation magnetic moment per Fe ion at room temperature.

netic moment $\langle\mu\rangle$. Therefore, constant ω means that $\langle\mu\rangle$ of iron in ZnFe_2O_4 is independent of Cu doping. It is well known that the NMR spectral intensity is proportional to $N\omega^{7/4} \propto N\langle\mu\rangle^{7/4}$, where N is the number of magnetic atoms. The NMR spectral intensity becomes proportional to magnetization $N\langle\mu\rangle$ when $\langle\mu\rangle$ is constant, as in this case. Since the observed NMR spectrum arises only from inverted ZnFe_2O_4 , the spectral intensity represents the magnetization of ZnFe_2O_4 produced in $\text{Zn}_{0.95-x}\text{Fe}_{0.05}\text{Cu}_x\text{O}$. The magnetization of ZnFe_2O_4 in the sample is proportional to that of the whole sample for varying Cu concentrations, as shown in the bottom figure, indicating the magnetic property observed in $\text{Zn}_{0.95-x}\text{Fe}_{0.05}\text{Cu}_x\text{O}$ is indeed that of the secondary phase. It appears that Cu doping into $\text{Zn}_{0.95}\text{Fe}_{0.05}\text{O}$ causes the formation of ZnFe_2O_4 nanoclusters with inverted spinel structure at low concentrations. This may be understood as follows: the addition of CuO in the processing stage appears to release oxygen, and this extra oxygen would then generate ZnFe_2O_4 locally. As the amount of ZnFe_2O_4 grows above 1% Cu doping, a portion of inverted zinc ferrite starts to turn normal.

Finally, we show the magnetization of $\text{Zn}_{0.94}\text{Fe}_{0.05}\text{Cu}_{0.01}\text{O}$ and ball-milled ZnFe_2O_4 as a function of temperature (Fig. 4). The transition temperature of the ball-milled ZnFe_2O_4 sample is 460 K, and the magnetization rises slowly below T_c as temperature is reduced; in contrast, the transition temperature of $\text{Zn}_{0.94}\text{Fe}_{0.05}\text{Cu}_{0.01}\text{O}$ is 550 K and the magnetization increases rather steeply below T_c . These differences may be attributed to the size difference of the two samples. The average grain size may be roughly estimated from the diffraction pattern using the Scherrer formula. The average grain size of ZnFe_2O_4 clusters in $\text{Zn}_{0.94}\text{Fe}_{0.05}\text{Cu}_{0.01}\text{O}$ was estimated to be larger than 100 nm, while that of the ball-milled ZnFe_2O_4 was approximately 20 nm. The ball-milled ZnFe_2O_4 showed superparamagnetic behaviors at

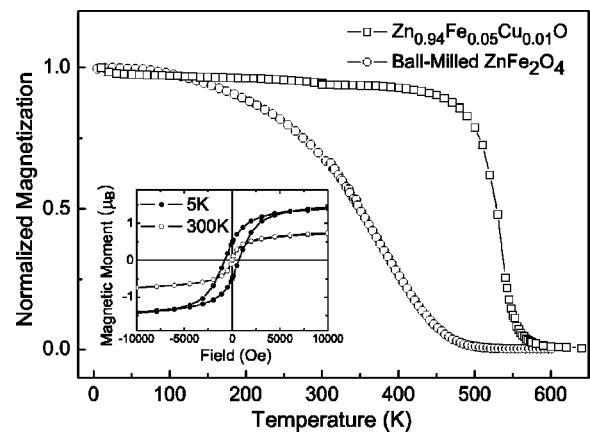


FIG. 4. The normalized magnetization of $\text{Zn}_{0.94}\text{Fe}_{0.05}\text{Cu}_{0.01}\text{O}$ (open square) and ball-milled ZnFe_2O_4 (open circle) is plotted as a function of temperature. Inset shows the hysteresis curve of ball-milled ZnFe_2O_4 , which is superparamagnetic.

room temperature, as the inset of Fig. 4 indicates. This is consistent with previous works on nanoparticles showing that the critical particle size, below which particles become a single domain is several tens of nanometers.¹³ The transition temperature of nanoparticles is also known to decrease with decreasing grain size.¹⁴ Thus, the size difference seems to bring about the differences in magnetic properties illustrated in Fig. 4.

This work was supported by KOSEF (2000-SRC), KISTEP (2003-HANARO), NRL Program and a grant from the Ministry of Science and Technology (MOST) of Korea.

¹S. A. Wolf, D. D. Awschalom, R. A. Buhrman, J. M. Daughton, S. von Molnar, M. L. Roukes, A. Y. Chichelkanova, and D. M. Treger, *Science* **294**, 1488 (2001).

²H. Ohno, *J. Magn. Magn. Mater.* **200**, 110 (1999).

³T. Dietl, H. Ohno, F. Matsukura, J. Cibert, and D. Ferrand, *Science* **287**, 1018 (2000).

⁴W. Prellier, A. Fouchet, and B. Mercey, *J. Phys.: Condens. Matter* **15**, R1583 (2003).

⁵K. Ueda, H. Tabata, and T. Kuwai, *Appl. Phys. Lett.* **79**, 988 (2001).

⁶S.-J. Han, T.-H. Jang, Y. B. Kim, B.-G. Park, J.-H. Park, and Y. H. Jeong, *Appl. Phys. Lett.* **83**, 920 (2003); K. Ando, *cond-mat/0208010*.

⁷S. W. Yoon, S.-B. Cho, S. C. We, S. Yoon, B. J. Suh, H. K. Song, and Y. J. Shin, *J. Appl. Phys.* **93**, 7879 (2003); S. Kolesnik, B. Dabrowski, and J. Mais, *ibid.* **95**, 2582 (2004).

⁸S.-J. Han, J. W. Song, C.-H. Yang, S. H. Park, J.-H. Park, Y. H. Jeong, and K. W. Rhie, *Appl. Phys. Lett.* **81**, 4212 (2002).

⁹C. N. Chinnasamy, A. Narayanasamy, P. Ponpandian, K. Chattopadhyay, H. Cuéroul, and J.-M. Greneche, *J. Phys.: Condens. Matter* **12**, 7795 (2000).

¹⁰E. A. Turov and M. P. Petrov, *Nuclear Magnetic Resonance in Ferro and Antiferromagnets* (Halsted, New York, 1972).

¹¹K. Sato and H. Kitayama-Yoshida, *Hyperfine Interact.* **136/137**, 737 (2001).

¹²M. S. Park and B. I. Min, *Phys. Rev. B* **68**, 224436 (2003).

¹³D. L. Leslie-Pelecky and R. D. Rieke, *Chem. Mater.* **8**, 1203 (1996).

¹⁴C. N. Chinnasamy, A. Narayanasamy, N. Ponpandian, R. J. Joseyphus, B. Jeyadevan, K. Tohji, and K. Chattopadhyay, *J. Magn. Magn. Mater.* **238**, 281 (2002).